JOC Article

An Exceptional Red Shift of Emission Maxima upon Fluorine Substitution

Frederik C. Krebs* and Holger Spanggaard

The Danish Polymer Centre, RISØ National Laboratory, P.O. Box 49, DK-4000 Roskilde, Denmark

frederik.krebs@risoe.dk

Received February 5, 2002

The effect of perfluorination on photophysical properties was investigated through synthesis and photophysical characterization of two isostructural donor−acceptor−donor dye molecules. The synthesis of two versatile fluorinated benzene compounds, 1,4-difluoro-2,5-diperfluorooctylbenzene (**1**) and 1,4-dibromo-2,5-difluoro-3,6-diperfluorooctylbenzene (**2**), is presented. The X-ray structure of **2** has been determined and shows that the perfluorinated octyl chains segregate from the benzene rings in the solid state, giving rise to a layered structure. The further synthesis through Suzuki coupling reactions using 4-formylbenzeneboronic acid with (**2**) and 1,4-dibromo-2,5-dioctylbenzene (**3**) gave, respectively, 1,4″-diformyl-2′,5′-difluoro-3′,6′-diperfluorooctyl-*p*-terphenylene (**4**) and 1,4″-diformyl-2′,5′-dioctyl-*p*-terphenylene (**5**). The condensation of the dialdehydes **4** and **5** with 9,10-phenanthrenequinone and ammoniumbicarbonate in glacial acetic acid gave the dye molecules 1,4″-bis(1*H*-phenanthro[9,10-*d*]imidazol-2-yl)-2′,5′-difluoro-3′,6′-diperfluorooctyl-*p*-terphenylene (**6**) and 1,4″-bis(1*H*-phenanthro[9,10-*d*]imidazol-2-yl)-2′,5′-dioctyl-*p*-terphenylene (**7**), respectively. The UV−vis spectra of the two molecules are nearly identical, whereas the fluorescence spectra are very different. Compound **7** shows blue fluorescence with little solvent dependence ($\lambda_{emission} = 410$ nm in THF, CH_2Cl_2, and hexane), whereas compound **6** shows a highly solvent-dependent emission wavelength ($\lambda_{emission} = 583$ nm in THF, $\lambda_{emission} = 560$ nm in CH_2Cl_2, and $\lambda_{emission} = 450$ nm in hexane). The fluorescence red shift of compound **6** in a series of solvents with different polarity is discussed using the Lippert−Mataga equation. Fluorescence lifetime and quantum yields were also determined. Ultraviolet photoelectron spectroscopy (UPS) was performed on thin films of compound **6** and **7** on a gold substrate. The observed ionization potential was 4.55 eV in both cases.

Introduction

The 1*H*-phenanthro[9,10-*d*]imidazol-2-yl group is worth considering as a substituent in the field of molecular materials. It has many desirable properties such as good stability, ease of introduction into any molecular system containing an aromatic aldehyde, use as a chromophore with high extinction coefficient, readily tuneable absorption wavelength, and fluorophoric properties and is desirable as a large planar synthetic building block in supramolecular chemistry. Aside from the early reports of its synthesis[1] straight from phenanthrenequinone and an aromatic aldehyde, the system has received little interest. Recently, the use of the 1*H*-phenanthro[9,10-*d*]-imidazol-2-yl group because of its supramolecular properties has been reported in a molecular tweezer system for explosives[2] and as a fluorophore in a superradiant laser dye[3] as a result of its photophysical properties. In the latter case it has been found that the HOMO resides on the 1*H*-phenanthro[9,10-*d*]imidazol-2-yl group and that the LUMO resides on the aromatic system to which the 1*H*-phenanthro[9,10-*d*]imidazol-2-yl group is attached. In this paper we describe the synthesis and photophysical properties of two new compounds of this class that are isostructural terphenylenes with 1*H*-phenanthro[9,10-*d*]-imidazol-2-yl groups. The central part of the terphenylene group was prepared in two versions, substituted with either hydrogen or fluorine, as shown in Scheme 1. The object of this paper is to compare the differences in properties obtained upon substitution of the hydrogen by fluorine.

Results and Discussion

Synthesis. The perfluoroalkylation of 1,4-dibromo-2,5-difluorobenzene using a procedure modified from that given in ref 4 with perfluorooctyliodide and copper dust in dry dimethylsulfoxide proceeds in very good yield to give **1**. In analogy with the bromination of pentafluorobenzene,[5] bromination of **1** in 65% oleum using $AlBr_3$ as a catalyst gives initially a heterogeneous mixture that after reflux for 6 h becomes homogeneous.[6] When con-

(1) (a) Krieg, B.; Manecke, G. *Z. Naturforsch., B*: *Anorg. Chem. Org. Chem. Biochem. Biophys. Biol.* **1967**, *22*, 132. (b) Neunhoeffer, O.; Krieg, B. Z. *Naturforsch., B*: *Anorg. Chem. Org. Chem. Biochem. Biophys. Biol.* **1966**, *21*, 536. (c) Cook, A. H.; Jones, D. *G. J. Chem. Soc.* **1941**, 278. (d) Steck, E. A.; Day, A. R. *J. Am. Chem. Soc.* **1943**, *65*, 452.

(2) Krebs, F. C.; Jørgensen, M. *J. Org. Chem.* **2001**, *66*, 6169−6173.

(3) Krebs, F. C.; Lindvold, L. R.; Jørgensen, M. *Tett. Lett.* **2001**, *42*, 6753−6757.

(4) McLoughlin, V. C. R.; Thrower, J. *Tetrahedron* **1969**, *25*, 5921−5940.

(5) Knunyants, I. L.; Yakobsen, G. G. *Synthesis of Fluoroorganic Compounds*; Springer-Verlag: Berlin, Heidelberg, New York, Tokyo, 1985.

10.1021/jo025592d CCC: $22.00
Published on Web 09/14/2002

SCHEME 1

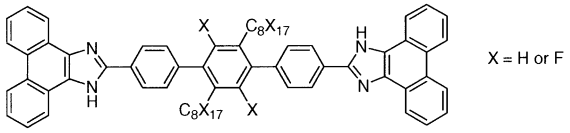

SCHEME 2

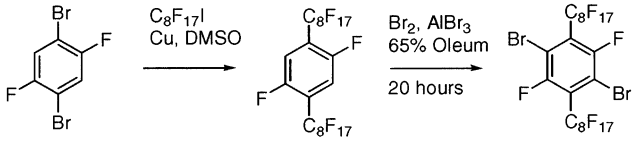

1 **2**

tinuing the reaction for another 14 h the dibrominated product **2** is obtained, as shown in Scheme 2.

The products are poorly soluble in common solvents such as methylenechloride, chloroform, and ether and moderately soluble in boiling toluene and boiling tetrahydrofurane. Characterization of the products using standard NMR techniques is essentially limited to ^{19}F NMR. Compound **1** contains only two protons and **2** contains none, which means that ^{1}H NMR gives little information and traditional ^{13}C NMR without special broadband C−F decoupling schemes gives rise to a myriad of signals due to the magnitude of the various carbon−fluorine coupling constants. The recording of ^{13}C NMR spectra of the neat compounds in the molten state (with a capillary containing DMSO-d_6) for 1−2 days gave only limited information. Elemental analysis was possible with addition of V_2O_5 to avoid combustion problems, and standard mass spectroscopy was also applied. A crystal structure was obtained that not only confirmed the molecular structure of **2** but also shed some light on the solid state behavior of the perfluorinated side chains, as few reports are available for this type of compound. The fluorinated side chains segregate, and a layered structure is observed, as shown in Figure 1.

Two comparable crystal structures could be found in the literature, one for a perfluorohexyl substituted aromatic compound and one for a perfluoroheptyl substituted aromatic system. Both examples show the same tendency for the perfluorinated side chains to segregate from the rest of the molecular system in the crystal.[7]

All attempts to perform ortholithiation or metal−halogen exchange on this series of molecules using standard bases (^{n}BuLi, ^{t}BuLi, ^{n}BuLi/TMEDA, PhLi) in common solvents (ether, THF, dioxane, ether/hexane) failed in our hands and we ascribe these problems to a lack of suitable solvents for these molecules at low temperature. The most successful attempt was obtained in ether/hexane (1:l) at 0 °C using ^{n}BuLi, where formylated products could be obtained after quenching with dimethylformamide. A significant degree of *n*-butylation was, however, also observed and believed to take place on both the aromatic carbon atoms and on the side chain

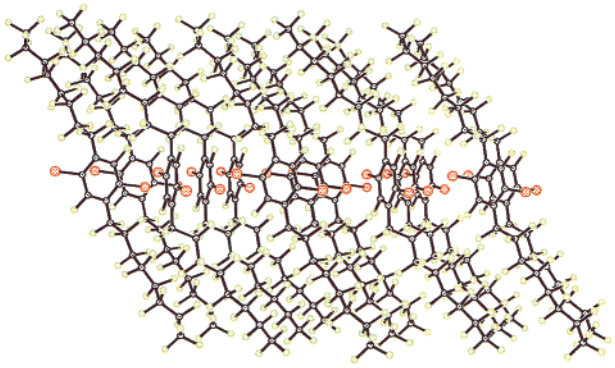

FIGURE 1. An illustration of the layered crystal structure observed for compound **2** (bromine atoms are red and fluorine atoms are green).

carbon atoms. This prompted us to try Suzuki-type reactions on compound **2**, and this was found to be possible under standard conditions using $(PPh_3)_2PdCl_2$ as catalyst and Na_2CO_3(aq) as the base in toluene at reflux temperature, as shown in Scheme 3. Further reaction of the dialdehydes **4** and **5** with ammoniumbicarbonate and phenanthrenequinone in glacial acetic acid gave **6** and **7**.

Photophysical Studies. The dye molecules **6** and **7** have very similar UV−vis spectra in both apolar (toluene) and polar (THF) solvents, as shown in Figure 2. The main differences between **6** and **7** in the absorption spectra are a slightly higher extinction coefficient, a small blue shift of the first maximum by 2 nm, and a small shoulder at the absorption edge for the fluorine compound (compound **6**). We believe that the smaller extinction coefficient arises because of a steric effect due to the fluorine atoms at the central benzene ring in the terphenylene system. Although neither **6** nor **7** is believed to acquire a planar conformation in the terphenylene system, the steric effect of the fluorine atoms in **6** makes the torsion angle between the central benzene ring and its aryl substituents larger than it is in **7**, as the geometry optimization shows (59° for **6** and 28° for **7**). Further evidence of a nonplanar geometry is found in the comparison of **6** and **7** with 4,4′-bis(1*H*-phenanthro[9,10-*d*]imidazol-2-yl)biphenyl, which is known to acquire a planar geometry leading to absorption maxima beyond 400 nm.[3]

Although both spectra are similar in both THF and toluene, it is noteworthy that the extinction coefficient for **7** is much more dependent on the polarity of the solvent. The extinction coefficient for both **6** and **7** decreases on going from polar THF to the less polar toluene, but while **6** only shows a slight decrease by about 10% the extinction coefficient of compound **7** decreases by a much more significant 40%, as can be seen from the data presented in Table 1. This is consistent with observations made for a system with a similar donor−acceptor-donor geometry.[11] The shoulder that is observed in **6** is slightly more pronounced in apolar solvents (vide supra). To substantiate the observations in the UV−vis spectra the isolated 1*H*-phenanthro[9,10-*d*]imidazol (**8**) was prepared and further comparison was made with 2-phenyl-1*H*-phenanthro[9,10-*d*]imidazol (**9**) and 2-(4-

(6) Attempts to isolate the product at this point gave mainly the monobrominated species; in our hands it was not possible obtain a pure sample free from **1** and **2**.

(7) Kromm, P.; Allouchi, H.; Bideau, J.-P.; Cotrait, M. *Mol. Cryst. Liq. Cryst. Sci. Technol., Sect. A* **1994**, *257*, 9. Kromm, P.; Bideau, J.-P.; Cotrait, M.; Destrade, C.; Nguyen, H. *Acta Crystallogr.* **1994**, *C50*, 112.

SCHEME 3

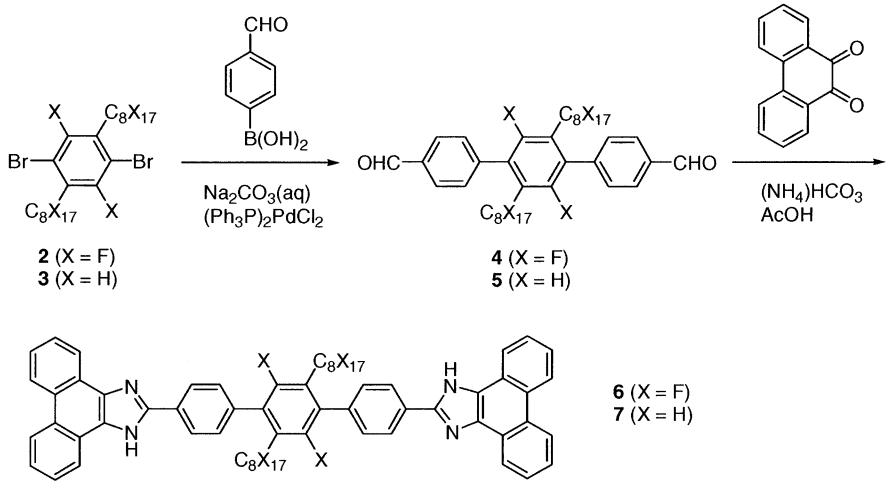

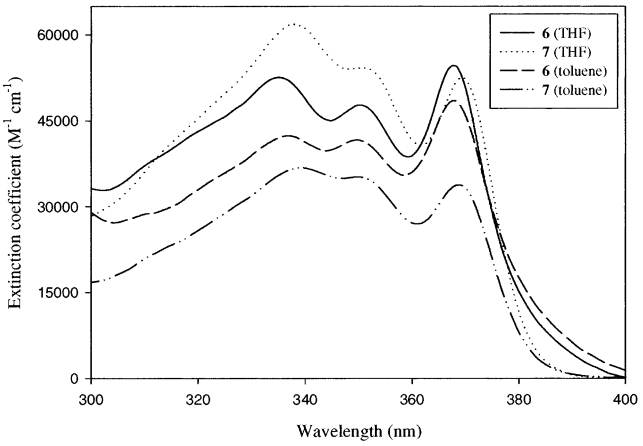

FIGURE 2. The UV−vis spectra of compounds **6** and **7** in THF and toluene.

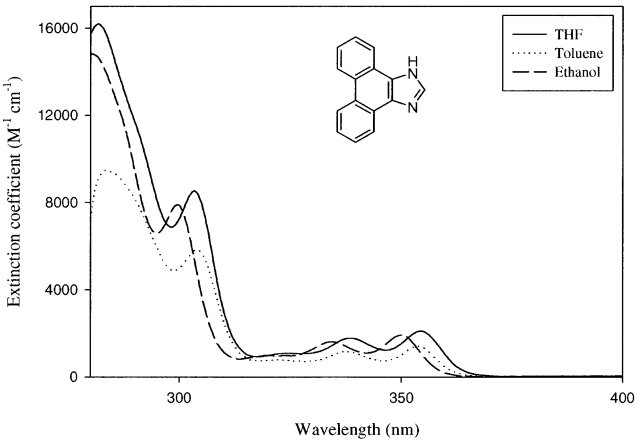

FIGURE 3. The UV−vis spectrum of the reference compound **8** in solvents of different polarity.

TABLE 1. λ_{max} (nm) Values and Associated Extinction Coefficients ϵ (M^{-1} cm^{-1}, in brackets) from UV−vis Spectra of 6 and 7 in THF and Toluene

6 (toluene)	**6** (THF)	**7** (toluene)	**7** (THF)
368 (48500)	368 (54500)	368 (33750)	370 (52250)
350 (41500)	350 (47750)	350 (35250)	350 (54250)
337 (42500)	335 (52500)	338 (36750)	338 (61750)

biphenyl)-1*H*-phenanthro[9,10-*d*]imidazol (**10**). Although the synthesis of 1*H*-phenanthro[9,10-*d*]imidazol has been reported, no analytical data can be found in the literature aside from the melting point and elemental analysis. The condensation reaction between phenanthrenequinone and an aromatic aldehyde in acetic acid containing a source of ammonium proceeds quite well, and this led us to attempt the condensation reaction between phenanthrenequinone and hexamethylenetetramine or aliphatic aldehydes that has been described. We however failed to produce the right product. Finally, the photochemical reaction of diphenylimidazole and iodine in benzene was employed, giving the isolated phenanthroimidazole moiety **8** as shown in Scheme 4. It is noteworthy that while many references including recent ones can be found, the NMR data have not been presented.[1,8] Therefore the data were included in the supplementary section.

SCHEME 4

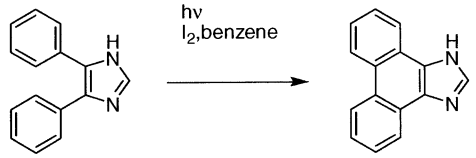

8

The UV−vis spectrum of **8** (doubly sublimed) shows features similar to that reported for phenanthro[9,10-*d*]-oxazole[9] except that there are weak transitions with extinction coefficients of the order of 1000−2000 M^{-1} cm^{-1} in the 320−350 nm range as shown in Figure 3 and Table 2. The observation of these transitions was substantiated by ZINDO calculations (vide supra).

The weak transitions in the 320−350 nm region were originally considered to be n−π* transitions, both because of their low intensity and because it has been reported that these transitions were n−π* and could be suppressed

(8) (a) Isikdag, I.; Ucucu, U.; Ozdemir, A.; Meric, A.; Ozturk, Y.; Aydin, S.; Ergun, B. *Boll. Chim. Farm.* **1999**, *138*, 453−456. (b) Purushothaman, E.; Rajasekharan-Pillai, V. N. *Indian J. Chem. B.* **1989**, *28*, 290−293. (c) Oda, K.; Sakai, M.; Tsujita, H.; Machida M. *Synth. Commun.* **1997**, *27*, 1183−1189.

(9) Padwa, A.; Ku, H.; Mazzu, A. *J. Org. Chem.* **1978**, *43*, 381−387.

(10) Baumann, W.; Bischof, H.; Fröhling, J. C.; Brittinger, C, Rettig, W.; Rotkiewicz, K. *J. Photochem. Photobiol., A* **1992**, *64*, 49.

(11) Strehmel, B.; Sarker, A. M.; Malpert, J. H.; Strehmel, V.; Seifert, H.; Neckers, D. C. *J. Am. Chem. Soc.* **1999**, *121*, 1226−1236.

TABLE 2. λ_{max} (nm) Values and Associated Extinction Coefficients ϵ (M^{-1} cm^{-1}, in brackets) from UV−vis Spectra of Compound 8 in EtOH, THF, and Toluene

EtOH	THF	toluene
350 (1900)	355 (2050)	354 (1400)
335 (1600)	338 (1750)	337 (1150)
320 (950)	325 (1050)	322 (750)
300 (7850)	303 (8500)	304 (5850)
280 (14800)	282 (16200)	283 (9450)

TABLE 3. λ_{max} (nm) Values and Associated Extinction Coefficients ϵ (M^{-1} cm^{-1}, in brackets) from UV−vis Spectra of 8, 9, and 10 in THF

8	**9**[a]	**10**[a]
355 (2050)	364 (10600)	372 (29850)
338 (1750)	347 (12200)	352 (29950)
325 (1050)	327 (22100)	340 (42650)
303 (8500)	314 (21400)	*b*

[a] Values taken from ref 3 and rounded to nearest 50. [b] It is noticeable that although no distinct peaks are observed there is a shoulder indicating the presence of at least one peak.

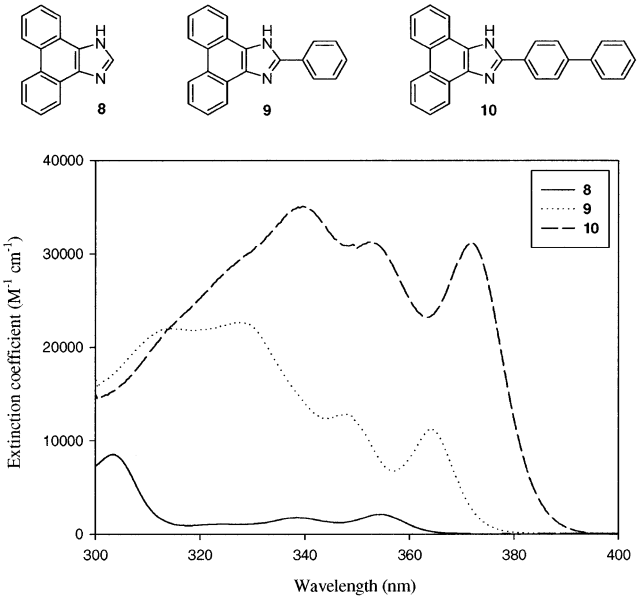

FIGURE 4. The absorption spectra of the reference compounds **8**, **9**, and **10** in THF.

in hydrogen donor solvents such as ethanol.[8b] As seen in Figure 3 and Table 2 the absorption spectrum in ethanol shows only minor changes in the magnitude of the extinction coefficient and a hypsochromic shift of 5 nm. The introduction of a phenyl or biphenyl substituent in the 2-position of the 1*H*-phenanthro[9,10-*d*]imidazol moiety as for compound **9**[3] and **10**[3] leads to a strong increase in the magnitude of the extinction coefficient, indicating $\pi-\pi^*$ character.

The UV−vis spectra show essentially the same features subjected to a bathochromic shift as summarized in Table 3. The hyperchromic shifts associated with all of the peaks are also given in Table 3, and the UV−vis spectra are shown in Figure 4. We therefore assume that the transitions in the 320−350 nm region are $\pi-\pi^*$ transitions.

In the emission spectra of the reference compounds (shown in Figure 5) fine structure is observed for **8** and

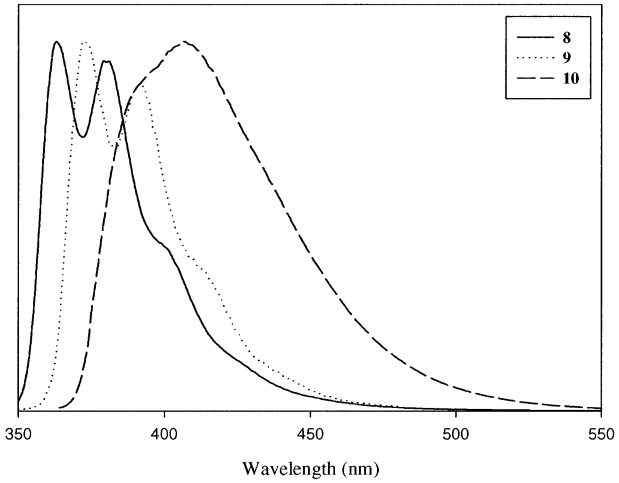

FIGURE 5. The emission spectra obtained for **8**, **9**, and **10** in THF under magic angle conditions. All spectra are normalized for easy comparison.

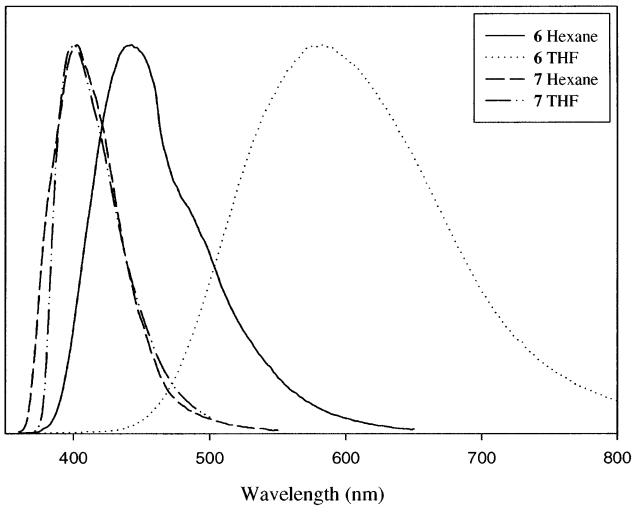

FIGURE 6. The emission spectra obtained for **6** and **7** in polar (THF) and nonpolar (hexane) solvents under magic angle conditions. All spectra are normalized for easy comparison. Notice the extreme polarity dependence of the emission maximum in the case of **6**.

9. Compound **9** exhibits a slight bathochromic shift in the emission as expected. Compound **10** however does not show fine structure, which could be indicative of solvent rearrangements and changes in the molecular geometry upon excitation. The emission spectrum of **10** is similar to the emission spectrum of **7** (Figure 6), and we interpret this as an indication that in both compounds the excitation is localized at the phenanthroimidazol moiety. Otherwise we would have expected an increased bathochromic shift in the absorption spectrum compared to that of **10**. This then supports the concept that upon excitation the phenanthroimidazol moiety can be subject to either a planarization or partial planarization with the phenylene ring upon which it is attached and with the central phenylene group. In the case of a local excitation the emission spectrum shows fine structure as found for **8** and **9**. In a more extended system like **10** a planarization event (or solvent rearrangement) during the transition takes place. The transition can thus still be considered as one of local character and the emission is now

lacking fine structure. Only two of the phenylene units in the terphenylene system are thus believed to be involved in the excitation and emission processes.

The emission spectrum of **6** and **7** in THF and hexane is shown in Figure 6. In all cases the spectra were broad and there was no sign of fine structure. The emission maximum of **6** showed a large red shift going from nonpolar to polar solvents. This is in marked contrast to the emission spectrum of **7**, which shows virtually no solvent dependence.

We ascribe this behavior to two different mechanisms. In the case of **7** we have a local excitation involving some rotation or planarization of the central phenylene moiety, which gives rise to a lack of fine structure in the emission spectrum. The solvent polarity dependence of the quantum yield for the emission in **7** only shows a slight decrease. For **6** the initial excitation can either be of the same local character as for **7** or it could be a direct charge-transfer transition connected to the shoulder in **6** that lies underneath the dominant $\pi-\pi^*$ transitions. However, the strongly electron-withdrawing perfluorinated central phenylene unit probably makes a different pathway available where some degree of charge transfer is possible, and the position of the emission maximum now shows a strong dependence on solvent polarity. Furthermore, the quantum yield for the emission process decreases severely when solvent polarity is increased, as expected.[11] Typically there is a difference between the ground state dipole and the excited state dipole of a molecule. Upon excitation the solvent molecules will rearrange according to the newly formed dipole vector and thereby stabilize the excited state. In general the more polar the solvent the more the excited state will be stabilized. The effect is an increased red shift of the emission spectrum in more polar solvents, which is described by the Lippert−Mataga equation,[10]

$$V_F = C_1 - \frac{1}{hc4\pi\epsilon_0}\frac{2}{a^3}\mu_e(\mu_e - \mu_g^{FC})\Delta f \qquad (1)$$

where C_1 is a constant, μ_e and μ_g^{FC} are the dipole moments in the excited and ground state, respectively, and FC denotes that the ground state has an unrelaxed Franck−Condon geometry. Δf is the solvent polarity and is given by eq 2 where ϵ is the dielectric constant and n is the optical refractive index.

$$\Delta f = \frac{\epsilon - 1}{2\epsilon + 1} - \frac{(n^2 - 1)}{(2n^2 + 1)} \qquad (2)$$

Equation 1 assumes the presence of a molecular dipole. However **6** does not have a dipole moment, since it contains a center of symmetry, but a quadrupole moment with a charge of -2δ on the central terphenylene unit and of $+\delta$ on each of the two 1*H*-phenanthro[9,10-*d*]-imidazol-2-yl groups. Despite the lack of a dipole moment the red shift of **6** in dichloromethane/hexane mixtures can be described by the Lippert−Mataga equation (see Figure 7). We speculate that because **6** is a rather large molecule its quadrupole moment can be approximated by two isolated dipole moments. This approximation is most valid around the 1*H*-phenanthro[9,10-*d*]imidazol-2-yl unit and the least valid around the center of the molecule (the terphenylene unit) where the two dipoles

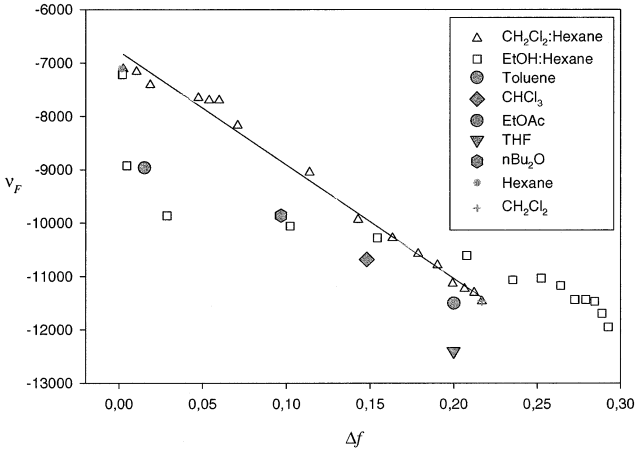

FIGURE 7. The Lippert−Mataga plot for compound **6** in dichloromethane/hexane mixtures (triangles with linear fit) and for ethanol/hexane mixtures (squares) showing a nonlinear relationship. Additionally the single points are obtained from solutions in pure solvents with different dielectric constants.

TABLE 4. Quantum Yields and Lifetimes at Emission Maximum (ns, in brackets) for Compounds 6 and 7 in Argon-Degassed Solvents

compound	CH_2Cl_2	ethanol
6	0.36 (4.4)	0.024 (1.10)
7	0.68 (1.2)	0.45 (0.85)

will cancel each other to some extent. This means that the observed red shift is less than should be expected if the dipoles were isolated. Strehmel et al. have also applied the Lippert−Mataga equation to molecules without a net dipole moment but, as in our case, with a quadrupole.[11] For **6** in ethanol/hexane mixtures ν_f is a nonlinear function of Δf, suggesting a specific interaction between ethanol and **6**, possibly H-bonding between ethanol and the amine or imine functionality on the 1*H*-phenanthro[9,10-*d*]imidazol-2-yl group. The effect of ethanol on **6** can also be seen in the quantum yields and lifetimes presented in Table 4.

In dichloromethane/hexane mixtures ν_f is a linear function of Δf with a slope of -21300 cm^{-1}. Individual points obtained for solutions in pure solvents were also obtained, and a linear fit to these data gave a slope of -19000 cm^{-1}.

The slope is relatively steep, indicating that the quadrupole moment in the excited state is substantially larger than the ground state quadrupole. Further, the slope is substantially steeper than that obtained for donor-π-acceptor molecules such as dialkylaminonaphthalenesulfonamides (-10600 cm^{-1}) and coumarins (-11300 cm^{-1})[12] but similar to the slope obtained for a series of donor-π-acceptor molecules forming intramolecular charge transfer states upon excitation, such as dimethylaminobenzonitriles (from -15000 to -24200 cm^{-1}) and dimethylaminobenzoic esters (-27200 cm^{-1}).[8] This suggests that there is a substantial charge transfer upon excitation. The ground state of **6** is expected to have a strong quadrupole due to the powerful electron-withdrawing effect of the fluorine atoms on the central

(12) Jager, W. F.; Volkers, A. A.; Neckers, D. C. *Macromolecules* **1995**, *28*, 8153.

terphenylene moiety. Semiempirical calculations on geometry optimized molecular structures (using MM2 with a CVFF force field[13]) of **6** and **7** using the ZINDO[13] program (developed by M. Zerner with INDO/1 parametrization using CIS) showed that the HOMO is located on the 1*H*-phenanthro[9,10-*d*]imidazol-2-yl group while the LUMO is located on the central benzene core in the terphenylene unit. Thus the effect of excitation is to transfer charge to the central part of the molecule, thereby increasing the existing quadrupole. The processes can be summarized in the following scheme shown below (taken from ref 11):

$$\mathrm{LE} \underset{\text{fluorescence}}{\overset{\text{absorption}}{\rightleftharpoons}} \mathrm{LE}^* \rightarrow \mathrm{CT}^* \underset{\text{absorption}}{\overset{\text{fluorescence}}{\rightleftharpoons}} \mathrm{CT}$$

In the case of compound **6** the emission comes from the excited charge transfer state (CT*) independent of the state it was in upon excitation. In compound **7**, however, there is no process that leads to the CT* state and emission comes solely from the locally excited state (LE*). The calculations also show that the HOMO and the LUMO of **7** are very similar to those of **6**. In the case of **7** however the charge transfer to the central terphenylene unit upon excitation is not stabilized by the inductive effect of the fluorine atoms and the quadrupole is expected to be much smaller for **7**, thus favoring the local excitation. By the same argument the ground-state quadrupole of **7** is expected to be smaller than that of **6**. Equation 1 shows that the emission frequency varies with the square of the excited-state dipole moment and has a linear dependence with respect to the ground-state dipole moment; **6** has the strongest excited state quadrupole and a much larger difference in charge distribution between the ground and excited state. Consequently **6** shows a much stronger red shift in the emission wavelength than **7**. When the emission spectra of **6** in hexane and CH_2Cl_2 (and THF) are compared, it is obvious that the latter is very broad, but it also seems that the shoulder in hexane (around 500 nm) is missing in CH_2Cl_2 (and THF). This may indicate that emission takes place from one state in hexane and another in CH_2Cl_2 (and THF).

To examine the possible presence of an excited state reaction, time resolved emission spectroscopy (TRES) was performed on **6** in CH_2Cl_2. The investigations showed a progressive red shift of the emission with time as expected. This is a consequence of increasing solvent reorientation around **6**. More importantly the spectra showed a slight broadening (FWHM) by about 400 cm^{-1} during the first 1−2 ns after excitation. This might indicate that a second state responsible for the broadening is appearing fairly quickly.[14] In the ground state most conjugated π-systems will try to maintain a planar structure, but in our case the conjugated system is forced out of the ideal planar arrangement as a result of the steric repulsions from the bulky perfluorooctyl substituents. Upon excitation the high degree of charge transfer effectively disrupts the conjugated system whereby the central terphenylene unit is free to rotate to minimize the steric repulsions—this mechanism is normally referred to as twisted intramolecular charge transfer or TICT.[15] We speculate that such a TICT mechanism may be responsible for the spectral broadening. The photoelectron spectroscopy data show that the ionization potentials are identical for **6** and **7**. The only difference is a slight shift of the energy levels to lower energies for compound **6**. Under the assumption that the samples are free from impurities and the crystallites are randomly oriented at the surface of the gold substrate, the Fermi levels in **6** and **7** align with the Fermi level of the gold substrate, making this observation possible (shown in figure S1 in the Supporting Information). It is also evident that the magnitude of the ionization potential is identical for **6** and **7**, but the relative position of the energy levels is indeed lower for **6** as a result of the inductive effect of the fluorine atoms. These results confirm the similarity of the experimental electronic structure in the solid state.

Conclusions

We have presented the synthesis of two isostructural donor−acceptor−donor dye molecules, one fully hydrogenated and one fluorinated on the acceptor part of the molecule. We show by photochemical means that while the electronic structure of the two compounds are very similar for the two compounds, as established by UV−vis and photoelectron spectroscopy, the emission properties are very different. The effects were very noticeable for the fluorinated molecule where the positions of hydrogen-to-fluorine substitution were chosen to stabilize the excited state. As expected this resulted in a large dependence of the emission maximum on the solvent polarity, whereas the compound containing only hydrogen showed no significant dependence on solvent polarity.

Experimental Section

All reagents were commercially available unless otherwise stated. 1,4-Dibromo-2,5-dioctylbenzene was prepared as described in ref 16, and 4-formylphenylboronic acid was prepared as described in ref. 17. The solubility of compound **6** in DMSO-d_6 at 440 K was too low to obtain a ^{13}C NMR spectrum. The ^1H and ^{19}F NMR spectra were obtained by long acquisition periods. High resolution (HRMS) mass spectrometry was performed using using a wavelength of 337 nm for matrix-assisted laser desorption ionization (MALDI). The peak at *m*/*z* 273.0393 of $[M - H_2O + H]^+$ ions of the matrix compound (2,5-dihydroxybenzoic acid, DHB) was used as an internal calibration standard.

2,5-Difluoro-1,4-bis(perfluorooctyl)benzene (1). Cu-bronze (50 g) was stirred in dry DMSO (400 mL, dried by distillation from CaH_2) and degassed with argon. Perfluorooctyl iodide (200 g, 0.366 mol) was added, and the mixture was heated on an oil bath (140 °C bath temperature). After 45 min 2,5-difluoro-1,4-dibromobenzene (47.5 g, 0.174 mol) was added, and the mixture was left overnight in the oil bath. The mixture was cooled to room temp for 2 h. A lower layer separated, which became solid. Aqueous ammonia (0.2 L) was added. and the supernatant was decanted. The solid lump was washed with several portions of aqueous ammonia. The lump was dissolved in boiling toluene (3 L) and filtered, giving a light yellow filtrate with a white precipitate. The mixture was cooled. The colorless product was filtered, washed with toluene

(13) *Insight II User Guide*, October 1995. Biosym/MSI: San Diego, 1995.
(14) Röcker, C.; Heilemann, A.; Fromherz, P. *J. Phys. Chem.* **1996**, *100*, 12172.
(15) Rettig, W. *Top. Cur. Chem.* **1994**, *69*, 253.
(16) Rehahn, M.; Schlueter, A.-D.; Feast, J. W. *Synthesis* **1988**, *5*, 386−388.
(17) Park, P. C.; Yoshino, K.; Tomiyasu, H. *Synthesis* **1999**, *12*, 2041−2044.

(2 × 500 mL) and methylene chloride (2 × 500 mL), and dried. This gave **1** as a colorless material in 76% yield (125 g): mp 111−112 °C; ^{1}H NMR (250 MHz, $CDCl_3$, 330 K, TMS) δ 7.5 (dd, ^3J(H,F) = 9 Hz, ^4J(H,F) = 7 Hz, 2H); ^{19}F NMR (235 MHz, $CDCl_3$, 330 K, C_6F_6) δ −122.2 (m, 4F), −118.7 (m, 4F), −117.7-(m, 16F), −110.6 (m, 2F), −105.9 (m, 4F), −77.2 (m, 6F). Anal. Calcd for $C_{22}H_2F_{36}$: C, 27.81; H, 0.21. Found: C, 27.91; H, 0.13.

1,4-Dibromo-2,5-difluoro-3,6-perfluorooctylbenzene (2). Aluminum foil (1 g) was cut into small pieces and placed in a 1 L round-bottomed flask with a large stirring bar. The flask was flushed with argon. Bromine (10 mL) was added in one portion, and the mixture was stirred vigorously under Ar until the aluminum had reacted (CAUTION!). The aluminum foil burns vigorously in the bromine vapor with a bright luminous flame, and care has to be taken that the aluminum pieces do not stick to the side of the flask but are kept stirring round. When the reaction has subsided oleum (60%, 300 mL) was added followed by bromine (70 mL, excess) and **1** (48 g, 0.05 mol). A condenser was fitted, and the mixture was stirred under Ar in an oil bath with a temperature of 40 °C. Initially the starting material floats inside the flask, but after 6 h the mixture becomes homogeneous. After 20 h the mixture was poured into ice (4 kg) and filtered. The product was washed with water (2 × 500 mL), $Na_2S_2O_6$(aq) (1 M, 2 × 500 mL) and recrystallized from toluene (1.5 L). This gave compound **2** in 82% yield (46 g): mp 131−132 °C; ^{19}F NMR (235 MHz, $CDCl_3$, 330 K, C_6F_6) δ −122.2 (m, 4F), −118.7 (m, 4F), −117.7 (m, 12F), −116.3 (m, 4F), −100.4 (m, 4F), −89.6 (m, 2F), −77.2 (m, 6F). Anal. Calcd for $C_{22}Br_2F_{36}$: C, 23.85; H. 0.00. Found: C, 23.83; H, 0.00.

4,4″-Diformyl-2′,5′-difluoro-3′,6′-perfluorooctylterphenylene (4). Compound **2** (5 g, 4.5 mmol), 4-formylphenylboronic acid (5 g, excess), Na_2CO_3 (14 g), water (150 mL), and toluene (300 mL) were mixed and degassed with argon. $(PPh_3)_2PdCl_2$ (300 mg, catalyst) was added, and the mixture was refluxed for 24 h. An additional amount of 4-formylphenylboronic acid (3 g, excess) was added with $(PPh_3)_2PdCl_2$ (300 mg, catalyst), and reflux continued for another 24 h. The mixture was cooled and left to crystallize. Filtering gave the product containing darkly colored catalyst decomposition products. The solids were boiled in toluene (400 mL) and filtered to give a near colorless solution that was left to crystallize, giving pure **4** as fine thin needle shaped crystals in 61% yield (3.2 g): mp 189−190 °C; ^{1}H NMR (250 MHz, $CDCl_3$, 330 K, TMS) δ 7.4 (d, ^3J(H,H) = 8 Hz, 4H), 8.0 (d, ^3J(H,H) = 8 Hz,, 4H), 10.1 (s, 2H); ^{13}C NMR (63 MHz, $CDCl_3$, 330 K, TMS) δ 129.9, 130.7, 137.0, 137.7, 191.8; ^{19}F NMR (235 MHz, $CDCl_3$, 330 K, C_6F_6) δ −122.2 (m, 4F), − 118.8 (m, 4F), −117.8 (m, 12F), −115.5 (m, 4F), −102.7 (m, 2F), −98.0 (m, 4F), −77.2 (m, 6F). Anal. Calcd for $C_{36}H_{10}F_{36}O_2$: C, 37.33; H, 0.87. Found: C, 37.13; H, 0.76.

4,4″-Diformyl-2,5-dioctylterphenylene (5). 1,4-Dibromo-2,5-dioctylbenzene (10 g, 21.7 mmol), 4-formylphenylboronic acid (10 g, excess), and Na_2CO_3 (10.6 g, 0.1 mol) were mixed in toluene (150 mL) and water (100 mL), and the mixture was degassed with argon. $(PPh_3)_2PdCl_2$ (350 mg, catalyst) was added, and the mixture was refluxed for 24 h. An additional portion of 4-formylphenylboronic acid (5 g, excess) and Pd-$(PPh_3)_4$ (350 mg, catalyst) were added, and the mixture was refluxed for 24 h. The reaction was stopped, and the organic phase was separated and concentrated. The crude oil was chromatographed on silica using toluene as eluent. Evaporation gave an oil that crystallized from petroleum, giving **5** in 25% yield (2.83 g): mp 61−63 °C; ^{1}H NMR (250 MHz, $CDCl_3$, 300 K, TMS) δ 0.8 (t, 6H), 1.2 (min, 20H), 1.5 (m, 4H), 2.6 (t, 4H), 7.1 (s, 2H), 7.5 (d, ^3J(H,H) = 8 Hz, 4H), 7.9 (d, ^3J(H,H) = 8 Hz, 4H), 10.1 (s, 2H); ^{13}C NMR (63 MHz, $CDCl_3$, 300 K, TMS) δ 14.8, 23.3, 29.8, 29.9, 30.1, 32.1, 32.5, 33.3, 130.3, 130.7, 131.4, 135.7, 138.3, 140.9, 148.9, 192.6; HRMS (MALDI, DHB): *m*/*z* calcd for $[C_{36}H_{46}O_2 + H]^+$ 511.3571, found 511.3592. Anal. Calcd for $C_{36}H_{46}O_2$: C, 84.66; H, 9.08. Found: C, 83.59; H, 8.88.

1,4-Diperfluorooctyl-2,5-bis(4-(1*H*-phenanthro[9,10-*d*]-imidazol-2- yl)phenyl)benzene (6). Compound **4** (0.67 g, 0.57 mmol) and 9,10-phenanthrenequinone (1 g. 4.8 mmol) were mixed in AcOH (50 mL), and NH_4HCO_3 (2 g, excess) was added. The mixture was heated to reflux, giving a light orange and clear solution. After 15 min the mixture becomes cloudy, and a light yellow precipitate forms. After 3 h the reaction was stopped, and the mixture was cooled overnight. The solid was filtered, washed with light petroleum, and recrystallized from toluene containing a little Et_3N. This gave **6** in 45% yield (0.4 g). DSC data for **6**: peak at 349.27 °C, ΔH = 76437 J mol^{-1}; ^{1}H NMR (250 MHz, DMSO-d_6, 440 K, TMS) δ 7.6−7.8 (m, 12H), 8.4 (d, ^3J(H,H) = 8 Hz, 4H), 8.6 (d, ^3J(H,H) = 8 Hz, 4H), 8.8 (d, ^3J(H,H) = 8 Hz, 4H), 13.1 (bs, 2H); ^{19}F NMR (235 MHz, DMSO-d_6, 440 K, C_6F_6 (sealed capillary)) δ −121.2 (m, 4F), −117.7 (m, 4F), −116.1 (m, 12F), 113.9 (m, 4F), 103.7 (m, 2F), −96.1 (m, 4F), −76.1 (m, 6F); HRMS (MALDI, DHB): *m*/*z* calcd for $[C_{64}H_{26}F_{36}N_4 + H]^+$ 1535.1655, found 1535.1644. Anal. Calcd for $C_{64}H_{26}F_{36}N_4$: C, 50.08; H, 1.71; N, 3.65. Found: C, 50.00; H, 1.64; N, 3.41.

1,4-Dioctyl-2,5-bis(4-(1*H*-phenanthro[9,10-*d*]imidazol-2-yl)phenyl)benzene (7). Compound **5** (0.4 g, 0.78 mmol), 9,10-phenanthrenequinone (0.6 g, 2.9 mmol), and NH_4HCO_3 (2 g, excess) were mixed in AcOH (50 mL) and heated to reflux for 3 h. After cooling the colorless product was filtered and washed with acetone. Recrystallization from toluene containing a little Et_3N gave **7** in 61% yield (0.42 g). DSC data for **7**: peak at 331.21 °C, ΔH = 94037 J mol^{-1}; ^{1}H NMR (250 MHz, DMSO-d_6, 300 K, TMS) δ 0.7 (t, 6H), 1.1 (m, 20H), 1.5 (m, 4H), 2.7 (t, 4H), 7.3 (s, 2H), 7.6−7.8 (m, 12H), 8.4 (d, ^3J(H,H) = 8 Hz, 4H), 8.6 (t, ^3J(H,H) = 8 Hz, 4H), 8.9 (d, ^3J(H,H) = 8 Hz, 4H), 13.5 (s, 2H); ^{13}C NMR (63 MHz, DMSO-d_6, 300 K, TMS) δ 13.8, 22.0, 28.4, 28.5, 28.8, 30.7, 31.2, 32.0, 121.8, 121.9, 122.4, 123.7, 124.1, 125.1, 125.2, 125.3, 125.9, 126.9, 127.0, 127.1, 127.5, 127.7, 128.9, 129.5, 130.7, 137.0, 137.2, 139.9, 142.0, 148.9; HRMS (MALDI, DHB): *m*/*z* calcd for $[C_{64}H_{62}N_4 + H]^+$ 887.5053, found 887.5170. Anal. Calcd for $C_{64}H_{62}N_4$: C, 86.64; H, 7.04; N, 6.32. Found: C, 86.33; H, 6.87; N, 6.22.

TABLE 5. Crystallographic Data for Compound 2

formula	$C_{22}F_{36}Br_2$
formula wt	1108.04
crystal system	monoclinic
space group	$P2_1/c$
Z	2
a, Å	22.089(8)
b, Å	5.863(2)
c, Å	11.966(5)
α, deg	90
β, deg	99.159(9)
γ, deg	90
V, Å^3	1529.9(10)
ρ, g cm^3	2.405
crystal dimensions, mm	0.75 × 0.75 × 0.006
type of radiation	Mo Kα
μ, cm^{-1}	2.890
T, K	120(2)
no. of reflections	18902
unique reflections ($I > 2\sigma$)	1706
R(F), R_w(F^2) all data	0.0992, 0.2788

Crystallography. General crystallographic data can be found in Table 5. The crystal of **2** was drawn directly from the mother liquour, coated with a thin layer of protecting oil, and mounted on a glass fiber using grease and transferred quickly to the cold stream of nitrogen on the diffractometer.

The crystals were very thin plates and this impaired the quality of the data. An almost complete sphere of reciprocal space was covered by a combination of several sets of exposure frames; each set with a different φ angle for the crystal and each frame covering a scan of 0.3° in ω. Data collection, integration of frame data, and conversion to intensities corrected for Lorenz, polarization, and absorption effects were

performed using the programs SMART,[18] SAINT,[18] and SADABS.[19] Structure solution, refinement of the structures, structure analysis, and production of crystallographic illustrations were carried out using the programs SHELXS97,[20] SHELXL97,[20] and SHELXTL.[21] The structure was checked for higher symmetry and none was found.[22] Crystallographic data (excluding structure factors) for the structure reported in this paper has been deposited with the Cambridge Crystallographic Data Centre as supplementary publication no. CCDC-177458. Copies of the data can be obtained free of charge on application to CCDC, 12 Union Road, Cambridge CB2 1EZ, UK (fax: (+44)-1223-336-033; e-mail: deposit@ccdc.cam.ac.uk).

Photophysical Methods. All measurements were performed using Spectrosolv grade solvents, and the solutions were degassed for 15 min with argon prior to use. Emission spectra and lifetimes were measured with an instrument comprised of a 450 W Xe lamp for steady-state measurements and a nanosecond flashlamp for lifetime measurements. The detecting system comprises a single photon counting PMT detector in a peltier cooled housing. All spectra where measured in a perpendicular geometry using 1-cm quartz cuvettes. Steady-state mesurements were obtained with a 1.8 nm band-pass and corrected. The quantum yield was determined using 9,10-diphenylanthracene in cyclohexane ($\phi_f = 1.00$, ref 23) as the fluorescence standard with refractive index and differential absorption corrections. In all cases lifetimes were single-exponential and determined using least-squares analysis as described by Straume.[24] All time-resolved measurements were conducted with 7.3 nm band-pass.

Photoelectron Spectroscopy. The samples for ultraviolet photoelectron spectroscopy measurements (UPS) were prepared by spin-coating a 1 μM solution of **6** and **7** in boiling chlorobenzene onto a freshly prepared polycrystalline gold surface. The samples were then dried in a vacuum oven at 50 °C for 24 h. The photoelectron spectra were recorded at the ASTRID storage ring at Aarhus University, Denmark. The beamline consists of an SX-700 monochromator and a hemispherical electron energy analyzer. An ESCA (electron spectroscopy for chemical analysis) scan of the samples was recorded first to check the cleanliness of the area where the incident photons illuminated the sample and to confirm the presence of the elements (C, N, and F for **6** and C and N for **7**). The photoelectrons were measured at an angle normal to the sample surface. The ESCA scans were performed with 800 eV photons and a resolution of 0.4 eV. The photoelectron spectra were recorded using 50 eV incident photons and a resolution of 0.2 eV. The experimental chamber was equipped with an ion gun, a mass spectrometer, and a gas dosing system. The sample holder was electrically isolated from the chamber, and the sample was kept at a potential of −9.5 V relative to the surrounding instrument. This serves to eliminate the contribution from the instrument work function at the low energy cutoff. A clean gold substrate was first entered and sputtered with ionized argon using an emission current of 22 mA and a potential of 3 kV. The sputtering was stopped after 1 h; subsequent measurements of the gold work function gave the reference value. The samples of **6** and **7** were introduced and the photoelectron spectra recorded. The onset and cutoff of the intensity normalized photoelectron spectra were used to compute the work function in the case of the pure gold substrate and the ionization potential and valence band edge in the case of the gold substrates containing the samples. The data are presented in Table 6.

TABLE 6. Data from Photoelectron Spectra for Au Substrate and Compounds 6 and 7

compound	E_F^{VB}	E_F^{VAC}	cutoff	Δ	IP
6	1.60	2.95	−45.45	−2.35	4.55
7	1.30	3.25	−45.45	−2.05	4.55

The gold work function, Φ_{Au}, was thus determined to be 5.3 eV. The position of the valence band edge for **6** and **7**, E_F^{VB}, was lower than the Fermi level of gold. The Fermi level in compounds **6** and **7** are thus situated in the forbidden band gap of the materials and the distance form the Fermi level of the samples to the vacuum level is given by the difference between the ionization potential, IP, and E_F^{VB}, giving E_F^{VAC}. The vacuum level shift, Δ, is thus obtained as $\Delta = E_F^{VAC} - \Phi_{Au}$. The vacuum level shift reflects how the molecules orient at the surface giving a dipole layer. The procedure employed in the analysis of the data has been reported.[25] See also the Supporting Information.

Acknowledgment. This work was supported by the Danish Technical Science Foundation of Denmark (STVF). We would like to express sincere gratitude to Ole Hagemann for assistance with the synthetic organic chemistry, Jan Alstrup for the DSC measurements, Mikkel Jørgensen for helpful discussion and NMR measurements, and Zheshen Li, Søren V. Hoffmann, and Philip Hofmann for technical support at the ASTRID storage ring and at the beamline.

Supporting Information Available: Experimental conditions and analytical data for **8**, including assignment of the NMR signals; excitation spectra for **6**−**10**. DSC data for **6** and **7**; an energy level diagram for **6** and **7** based on the photoelectron spectroscopy experiment. This material is available free of charge via the Internet at http://pubs.acs.org.

JO025592D

(18) SMART and SAINT; Area-Detector Control and Integration Software; Siemens Analytical X-ray Instruments Inc.: Madison, WI, 1995.

(19) Sheldrick, G. M. Empirical absorption program (SADABS) written for the Siemens SMART platform.

(20) Sheldrick, G. M. SHELX-97; Program for structure solution and refinement. 1997.

(21) Sheldrick, G. M. SHELXTL95; Siemens Analytical X-ray Instruments Inc.: Madison, WI, 1995.

(22) Spek, A. L. *Acta Crystallogr.* **1990**, *A46*, C-31.

(23) Ware, W. R.; Rothman, W. *Chem. Phys. Lett.* **1976**, *39*, 449−453.

(24) Straume, M.; Fraiser-Cadoret, S. G.; Johnson, M. L. In *Topics in Fluorescence Spectroscopy*; Lakowicz. J. R., Ed.; Plenum Press: New York, 1991; Vol. 2, pp 177−240.

(25) Salaneck, W. R.; Lögdlund, M.; Fahlman, M.; Greczynski, G.; Kugler, Th. *Mater. Sci. Eng.* **2001**, *R34*, 121−146.